The Journal of Headache and Pain

RESEARCH

Open Access

Disrupted topologic efficiency of white matter structural connectome in migraine: a graph-based connectomics study

Yanliang Mei[1†], Dong Qiu[1†], Zhonghua Xiong[1], Xiaoshuang Li[1], Peng Zhang[1], Mantian Zhang[1], Xue Zhang[2,3], Yaqing Zhang[1], Xueying Yu[1], Zhaoli Ge[4], Zhe Wang[5], Binbin Sui[2*], Yonggang Wang[1*] and Hefei Tang[1*]

Abstract

Objective To delineate the structural connectome alterations in patients with chronic migraine (CM), episodic migraine (EM), and healthy controls (HCs).

Background The pathogenesis of migraine chronification remains elusive, with structural brain network changes potentially playing a key role. However, there is a paucity of research employing graph theory analysis to explore changes in the whole brain structural networks in patients with CM and EM.

Methods The individual structural brain connectome of 60 patients with CM, 34 patients with EM, and 39 healthy control participants were constructed by using deterministic diffusion-tensor tractography. Graph metrics including global efficiency, characteristic path length, local efficiency, clustering coefficient, and small-world parameters were evaluated to describe the topologic organization of the white matter structural networks. Additionally, nodal clustering coefficient and efficiency were considered to assess the regional characteristics of the brain connectome. A graph-based statistic was used to assess brain network properties across the groups.

Results Graph theory analysis revealed significant disruptions in the structural brain networks of CM patients, characterized by reduced global efficiency, local efficiency, and increased characteristic path length compared to HCs. Additionally, CM patients exhibited significantly lower local efficiency than EM patients. Notably, the CM group demonstrated marked reductions in local clustering coefficient and nodal local efficiency in the frontal and temporal regions compared with the healthy control group and EM group. Nodal local efficiency can effectively distinguish CM from EM and HCs. Moreover, the disrupted topologic efficiency was significantly associated with attack frequency and MIDAS score in patients with migraine after Bonferroni correction.

†Yanliang Mei and Dong Qiu contributed equally to this work as the first author.

*Correspondence:
Binbin Sui
reneesui@163.com
Yonggang Wang
w100yg@gmail.com
Hefei Tang
13466537763@139.com
Full list of author information is available at the end of the article

Conclusion Decreased structural connectivity in the frontal and temporal regions may serve as a neuroimaging marker for migraine chronification and disease progression, providing valuable insights into the pathophysiology of chronic migraine.

Keywords Migraine, Structural connectivity, Diffusion tensor imaging

Introduction

Migraine is a prevalent brain dysfunction disease, characterized by recurrent, moderate to severe headache accompanied by photophobia, phonophobia, nausea and vomiting [1, 2]. The global migraine prevalence is about 14%, imposing a substantial economic burden on both individuals and society [3, 4]. About 3% of patients with episodic migraine (EM) will be converted into chronic migraine (CM) every year [5]. CM is defined as headache exceeding 15 days per month, of which migraine-like headache is greater than 8 days, persisting for more than three consecutive months [6].

Despite extensive research, the precise pathophysiological mechanisms underlying the chronification of migraine remain elusive [6, 7]. Risk factors such as anxiety, depression, obesity, and excessive use of acute analgesic have been associated with the progression of EM to CM [8, 9]. Neuroimaging studies suggest that both EM and CM may be linked to dysfunctions within neural networks that span multiple cortical and subcortical brain regions [10, 11]..

Recent studies utilizing diffusion tensor imaging (DTI) have highlighted extensive micro-structural changes in white matter among patients with migraine, especially those with CM [12–14]. The human brain functions as an intricate network, where advanced neuroimaging techniques, coupled with graph-based analyses, allow for the detailed examination of the brain's structural and functional connectomes [15]. This brain network primarily comprises interconnected nodes and edges, offering valuable insights into the pathogenesis of neurological disorders, including migraine [16].

Previous studies have primarily focused on alterations in functional connectivity network properties in migraine patients [17, 18]. However, there is a paucity of research employing graph theory analysis to explore changes in the whole brain structural networks in patients with CM and EM. Additionally, it remains unclear whether the topological efficiency of the white matter structural connectome within neural circuits involved in pain and emotion modulation correlates with migraine chronification and disease progression.

The primary objective of this study is to investigate the changes in white matter micro-structure and brain network abnormalities in patients with EM and CM using structural connectomics. By identifying the potential alterations in white matter topological efficiency underlying migraine chronification, this study aims to elucidate the relationship between structural connectivity efficiency and clinical characteristics of migraine.

Methods

Participants

The research was carried out using a cross-sectional design and was an observational study. One hundred and thirty-three participants, including 60 patients with CM, 34 patients with EM and 39 healthy controls (HCs), were consecutively enrolled from the headache outpatient unit at Beijing Tiantan Hospital (Capital Medical University) from October 2020 to March 2023. Patients were considered for inclusion based on the following criteria: The following criteria must be met: 1) a diagnosis of EM or CM (all patients had migraine without aura) according to the International Classification of Headache Diseases, Third Edition (ICHD-3) [19]; 2) 16–65 years of age; 3) the ability to perform a magnetic resonance imaging (MRI) scan effectively; and 4) the absence of preventive treatment for a period of at least three months. When it came to patients and HCs, the general exclusion criteria were as follows: 1) when combined with other types of primary headache and pain disorders; 2) when pregnant or breastfeeding; 3) when combined with other neurological, cardio-cerebrovascular, and endocrine system diseases; 4) any history of drug or alcohol abuse; 5) a first-degree relative who suffers from headaches; 6) improper quality of MRI data (significant susceptibility artefact or incomplete raw MRI data); and 7) significant brain lesions or white matter hyperintensities (Fazekas score greater than 1, especially at the level of the lateral ventricular body).

Demographic data and neuropsychological tests

Demographics, body mass index (BMI), headache disease duration (years), Visual Analogue Scale (VAS), Patient Health Questionnaire-9 (PHQ-9) scores, Headache Impact Test-6 (HIT-6) scores, Generalized Anxiety Disorder-7 (GAD-7) scores and Pittsburgh Sleep Quality Index (PSQI) scores were collected in all patients. Symptoms of depression and anxiety were assessed using the GAD-7 and the PHQ-9, respectively. The PSQI proved to be a valuable instrument in assessing sleep patterns and quality. Additionally, the HIT-6 was utilized to evaluate

the severity of headaches. The PHQ-9 was frequently employed as a screening tool for depression, with a suggested threshold score of 10 [20]. On the GAD-7, scores of 10 or greater were indicative of generalized anxiety disorder [21]. Poor sleep quality was defined as a PSQI score of seven or higher [22].

Approval of the local ethics committee of Beijing Tiantan Hospital, Capital Medical University (number: KY2022-044) granted this sub-study of the ongoing China HeadAche DIsorders RegiStry Study (CHAIRS, unique identifier: NCT05334927) designation. In adherence to the tenets outlined in the Declaration of Helsinki, prior to their involvement, every participant provided informed consent.

MRI acquisition

At the National Neurological Center of Beijing Tiantan Hospital, 3D T1 structural and diffusion MRI data were acquired using a GE 3.0 Tesla MR scanner (Signa Premier, GE Healthcare) equipped with a 48-channel head coil. The participants were instructed to remain motionless with their eyes closed during the MRI acquisition. All the following parameters were utilized in order to acquire T1 structural images: The MP-RAGE sequence has a preparation time of 880 ms, an acquisition time of four minutes, a recovery time of 400 ms, a field of view of 250×250 mm^2, an acceleration factor of 2, a flip angle of 8°, slices of 192, and a spatial resolution of $1\times1\times1$mm^3. The DTI parameters that were utilized in this study were as follows: the repetition time was set at 5285 ms, the data matrix was set at 104×104, the echo time was set at 85 ms, the slice thickness was set at 2 mm, the field of view was set at 208×208 mm^2, the resolution was set at $2.0\times2.0\times2.0$ mm^3, the number of slices was 78. The diffusion MRI data include 9 images of $b=0$, 50 gradient directions with a b-value of 1000 s/mm^2 and 50 gradient directions with 2000s/mm^2 under the anterior-to-posterior phase encode direction. Additionally, we acquired 4 images of $b=0$ and 3 gradient directions with 2000s/mm^2 under the posterior-to-anterior phase encode direction.

Data preprocessing procedure

Analyses were performed by two observers (YL M, D Q) respectively. Briefly, the preprocessing procedure for the DTI data included eddy current and motion artifact correction, estimation of the diffusion tensor, and calculation of the fractional anisotropy (FA). Before pre-processing, two expert neuroradiologists visually inspected the DTI image to screen for noisy artifacts. Images were processed by using the FMRIB software library (FSL, version 6.0.1; http://www.fmrib.ox.ac.uk/fsl). The *dcm2niigui* tool was used to convert the DICOM format of all diffused data into NIFTI format. The *topup* tool was applied for estimating and correcting susceptibility induced distortions by using anterior to posterior encoding direction and posterior to anterior phase-encoding direction. We used the *eddy_openmp* command to correct head motion and eddy current distortions. Brain masks from the *b0* image of each participant was created by using FSL's *BET* (Brain Extraction Tool). The FSL toolbox *DTIFIT* fits the pre-processed image based on a diffusion tensor model to yield FA values.

Network Construction

White matter tractography: We employed the Fiber Assignment by Continuous Tracking (FACT) method available in Diffusion Toolkit (http://www.trackvis.org/dtk/) for white matter fiber tracking [23]. Tracts in the diffusion-tensor imaging were generated by seeding voxels with FA values greater than 0.2 to perform whole-brain fiber tracking. For each seed, which consisted of eight seeds per voxel, a streamline was initiated. Tracking was terminated if the tracking angle exceeded 45 degrees or the FA value of the traversed voxel fell below 0.2 [24].

Network node definition: For the network analysis, we defined nodes using the Automated Anatomical Labeling (AAL) template [25] consisting of 90 brain regions after excluding the cerebellum. Initially, individual T1-weighted images were registered to the B0 DTI image space. The transformed T1-weighted images were then non-linearly normalized to the ICBM152 T1 template in the MNI standard space [26]. Subsequently, the AAL template was transformed from the MNI space to the individual DTI space using the inverse transformation, establishing the nodes for the structural connectome network in the individual's brain space.

Network edge definition: Edges in the DTI structural connectome network were defined based on the presence of at least three white matter fiber tracts between two brain regions [27]. Only direct connections between two regions of interest (ROIs) were counted if the fiber passes through both ROIs without being interrupted by other regions. Notably, the mean FA values of white matter fibers between two brain regions was considered the weight of the network edge [24, 28]. Consequently, each participant's structural connectome network comprised a weighted network of 90 nodes, represented as a symmetric 90×90 matrix based on FA values.

Statistical analysis

All clinical data were analyzed using Stata 15.0 software (StataCorp LLC, TX, USA). Continuous variables (ages, BMI) are reported as mean ± standard deviation (SD) or median with interquartile range and analyzed by the independent sample t-test, Mann–Whitney test, or one-way analysis of variance (One-way ANOVA) as

appropriate. The chi-square test was used to compare differences between genders. P-values < 0.05 were considered statistically significant. For analyses involving multiple comparisons, false discovery rate (FDR) correction was applied. The following graph metrics were evaluated in order to provide a description of the topologic organization of the white matter structural networks: global efficiency, characteristic path length, local efficiency, clustering coefficient, and small-world parameters. Moreover, nodal clustering coefficient and efficiency were taken into account when considering regional characteristics of the brain connectome. Gretna (http://www.nitrc.org/projects/gretna/) was utilized for all the network analyses, and BrainNet Viewer (http://www.nitrc.org/projects/bnv/) was utilized for the visualization of the results. Using age and gender as covariates, a general linear model was carried out in order to ascertain the differences that exist between the groups in terms of global and regional network metrics. The FDR correction was utilized in order to rectify the multiple comparisons that were obtained for the regional properties.

We utilized a network-based statistic (NBS) approach to identify the distinct connected subnetwork (component) with varying structural connections between the patients and healthy control groups [29]. The NBS analysis was conducted with edge-wise t-tests, applying an edge-level significance threshold of $p < 0.05$. Statistical significance was determined after 5,000 permutations, and subnetworks with a corrected component-level $p < 0.05$ were considered statistically significant. In order to assess the potential discriminatory capability of the network metrics among distinct groups, a receiver operating characteristic curve (ROC) analysis was conducted on those metrics that exhibited statistically significant group differences. Pearson correlation analyses were conducted between the network metrics showing significant group differences and the clinical scores within the patient group. Bonferroni correction was applied to account for multiple comparisons in these correlation analyses.

Results

Demographics and clinical characteristics

We recruited 152 participants with 69 patients with CM, 37 participants with EM, and 46 HCs in our initial cohort. Following quality control measures, nine CM participants were excluded due to poor MRI data quality ($n = 3$) and significant white matter hyperintensities ($n = 6$). Similarly, three EM participants were excluded for poor MRI data quality ($n = 2$) and white matter hyperintensities ($n = 1$). Seven HCs were excluded due to poor MRI data quality ($n = 3$) and existing white matter hyperintensities ($n = 4$) (Fig. 1). There were no differences in age, gender ratio and BMI found between the groups. For the clinical characteristics of patients with migraine, CM group showed higher attack frequency, MIDAS score, GAD-7 score, and PHQ-8 score (Table 1).

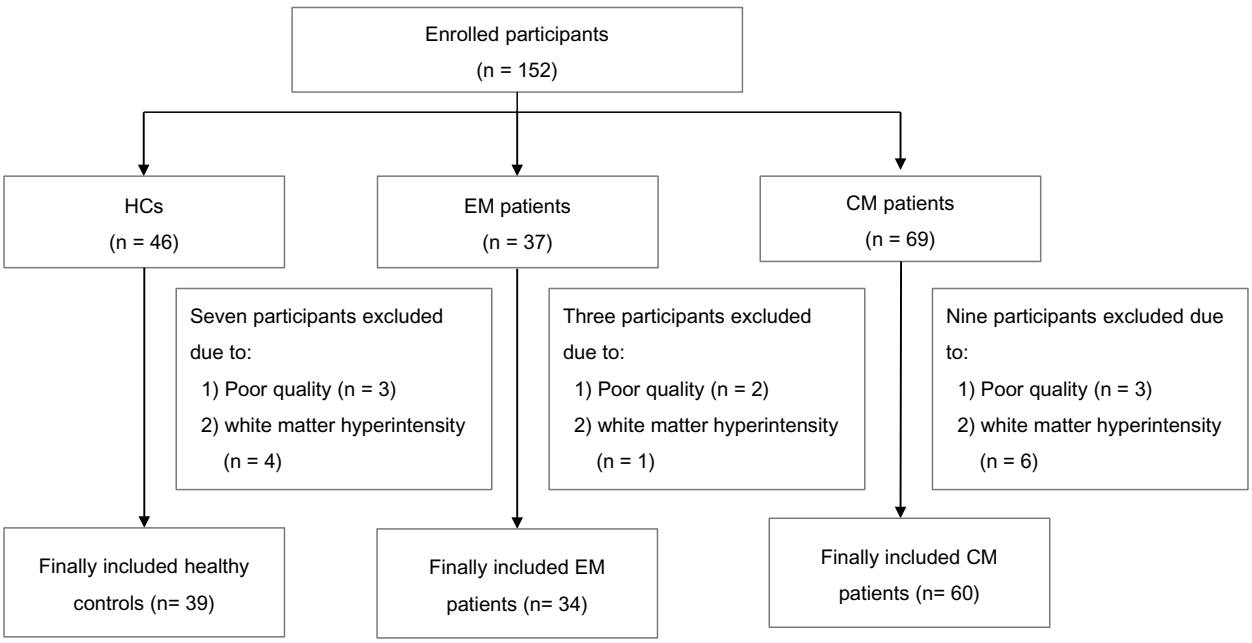

Fig. 1 Flowchart of the process for participant inclusion

Table 1 Demographic and clinical data

	Controls ($n=39$)	EM ($n=34$)	CM ($n=60$)	*P* value
Ages, years	34.97 ± 9.91	36.79 ± 13.9	39.37 ± 14.19	0.25[a]
BMI	22.76 ± 3.43	24.06 ± 4.13	22.89 ± 3.67	0.26[a]
Gender (female/male)	23/16	21/13	44/16	0.28[b]
Attack frequency (days/month)	/	6 (4)	25 (15)	< 0.001[c]
Disease duration (years)	/	11.5 (16)	16(19)	0.11[c]
Headache intensity (VAS)	/	6.67 ± 1.34	7.21 ± 1.50	0.08[d]
MIDAS score	/	50 (49)	100 (112)	< 0.001[c]
HIT-6 score	/	64 (11)	66 (8)	0.21[c]
PHQ-9 score	/	4 (6)	11 (10)	< 0.001[c]
GAD-7 score	/	3 (5)	8 (10)	< 0.001[c]
PSQI score	/	8 (6)	11 (9)	0.06[c]

EM Episodic migraine, *CM* Chronic migraine, *BMI* Body mass index, *VAS* Visual analogue scale, *HIT-6* Headache Impact Test-6, *PHQ-9* Patient Health Questionnaire-9, *GAD-7* Generalized Anxiety Disorder-7, *PSQI* Pittsburgh Sleep Quality Index

[a] One-way ANOVA,

[b] Chi-square test,

[c] Mann–Whitney U test,

[d] Independent samples t test

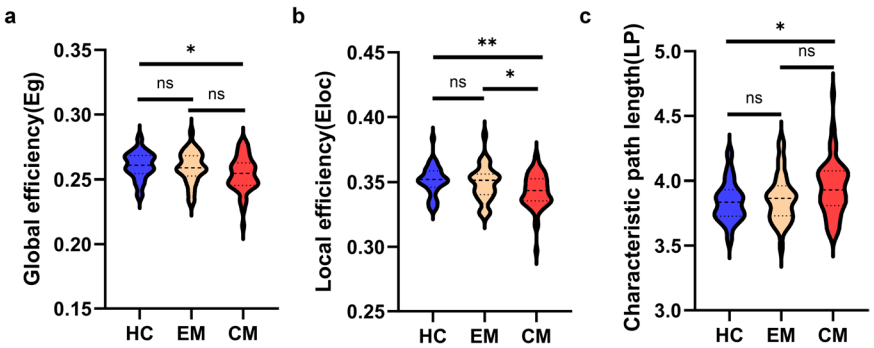

Fig. 2 Violin plots depicting group differences in global efficiency (**a**), local efficiency (**b**), and characteristic path length (**c**) of white matter structural FA networks. * $p<0.05$, ** $p<0.01$

Structural brain networks: global network properties

The global topologic network properties of the HCs, EM and CM groups were analyzed and reported in Fig. 2. When compared with healthy control subjects, patients with CM showed decreased global efficiency ($p=0.02$) and local efficiency ($p<0.01$). Characteristic path length was increased in patients with CM compared to HCs ($p=0.02$). When compared with HCs, patients with EM showed no significant group difference in global efficiency, local efficiency, and characteristic path length. When compared with patients with EM, patients with CM showed decreased local efficiency ($p=0.03$).

Structural brain networks: local network properties

When compared with HC group, we identified regions with less local clustering coefficient in the EM group in left middle frontal gyrus ($p<0.05$, corrected). Moreover, in comparison to the HC group, CM group showed less local clustering coefficient in left middle frontal gyrus and right dorsolateral part of the superior frontal gyrus ($p<0.05$, corrected). Additionally, compared with EM group, CM group showed less local clustering coefficient in right dorsolateral part of the superior frontal gyrus ($p<0.05$, corrected) (Fig. 3).

For the nodal local efficiency, compared with HC group, patients with EM showed significantly lower nodal local efficiency in right dorsolateral part of the superior frontal gyrus and left gyrus rectus; patients with CM showed significantly lower nodal local efficiency in that included the following regions: right dorsolateral part of the superior frontal gyrus, left gyrus rectus, right middle frontal gyrus, left opercular part of the inferior frontal gyrus, left hippocampus and left inferior temporal gyrus ($p<0.05$, corrected). Lastly,

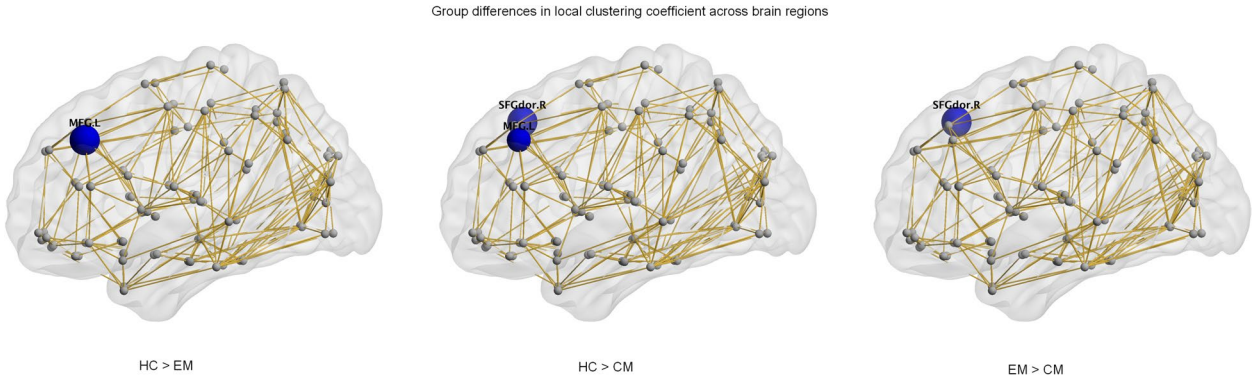

Fig. 3 The distribution of the brain regions, left (L) and right (R), with significantly lower local clustering coefficient in the different groups. The regions with significant group differences (HC > EM, HC > CM EM > CM; $p < 0.05$, corrected) were colored in blue. And *p*-values for each significant region are as follows: *p*-value of MFG.L in HC > EM = 0.0018, *p*-value of SFGdor.R in HC > CM = 0.000015, *p*-value of MFG.L in HC > CM = 0.0006, *p*-value of SFGdor.R in EM > CM = 0.002. MFG.L = left middle frontal gyrus, SFGdor.R = right dorsolateral part of the superior frontal gyrus

when compared with EM group, CM group showed significantly lower nodal local efficiency in right middle frontal gyrus, left opercular part of the inferior frontal gyrus, left hippocampus and left inferior temporal gyrus ($p < 0.05$, corrected) (Fig. 4).

Structural brain networks: network-based statistic

The NBS analysis was performed to explore the connected sub-network (component) with altered FA values with gender and age as covariates. When compared with HC group, EM group showed one decreased component of FA values with 4 nodes and 3 connections that included the following regions: right angular gyrus, right insula, right parahippocampal gyrus, and right lingual gyrus (corrected $p = 0.01$). When compared with HC group, CM group showed one decreased component of FA values with 16 nodes and 15 connections that included the subcortical nuclei (bilateral thalamus, basal ganglia) and cortical regions (corrected $p = 0.0001$). When compared with EM group, CM group showed one decreased component of FA values with 4 nodes and 3 connections that included the following regions: right orbital part of the middle frontal gyrus, right orbital part of the inferior frontal gyrus, right middle temporal gyrus, and right cuneus (corrected $p = 0.01$) (Fig. 5).

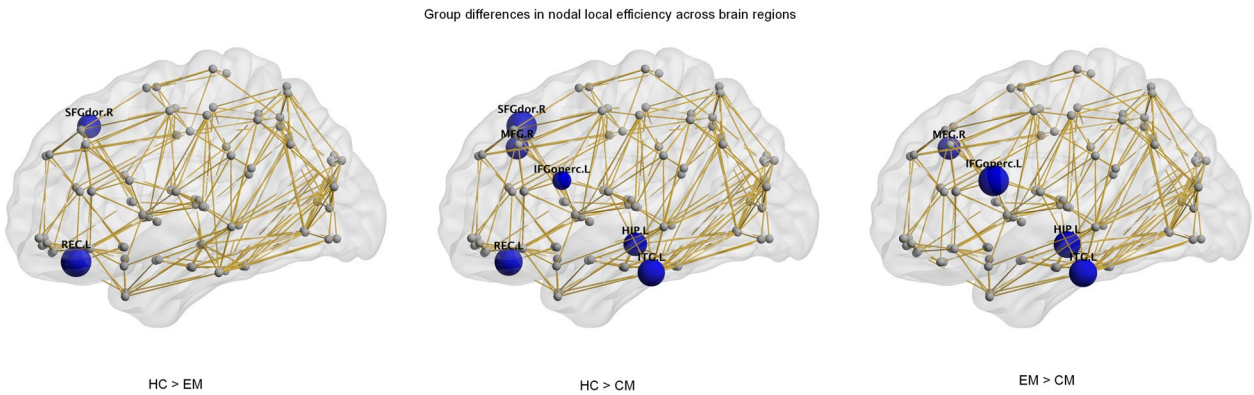

Fig. 4 The distribution of the brain regions, left (L) and right (R), with significantly lower nodal local efficiency in the different groups. The regions with significant group differences (HC > EM, HC > CM EM > CM; $p < 0.05$, corrected) were colored in blue. And *p*-value of SFGdor.R in HC > EM = 0.01, *p*-value of REC.L in HC > EM = 0.008, *p*-value of SFGdor.R in HC > CM = 0.0001, *p*-value of MFG.R in HC > CM = 0.004, *p*-value of IFGoperc.L in HC > CM = 0.01, *p*-value of REC.L in HC > CM = 0.0006, *p*-value of HIP.L in HC > CM = 0.003, *p*-value of ITG.L in HC > CM = 0.0008, *p*-value of MFG.R in EM > CM = 0.01, *p*-value of IFGoperc.L in EM > CM = 0.001, *p*-value of HIP.L in EM > CM = 0.004, *p*-value of ITG.L in EM > CM = 0.002. SFGdor.R = right dorsolateral part of the superior frontal gyrus, REC.L = left gyrus rectus, MFG.R = right middle frontal gyrus, IFGoperc.L = left opercular part of the inferior frontal gyrus, HIP.L = left hippocampus, ITG.L = left inferior temporal gyrus

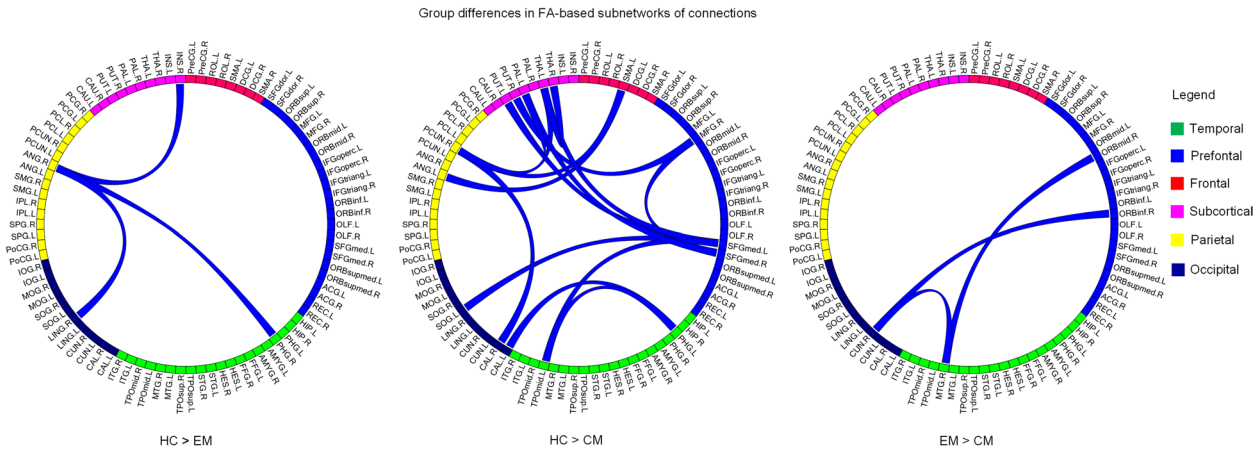

Fig. 5 The Connection graphs show the disrupted structural connections in the different groups identified by using NBS analysis. The blue curves indicate the lower FA values between the two regions (HC > EM, HC > CM, EM > CM)

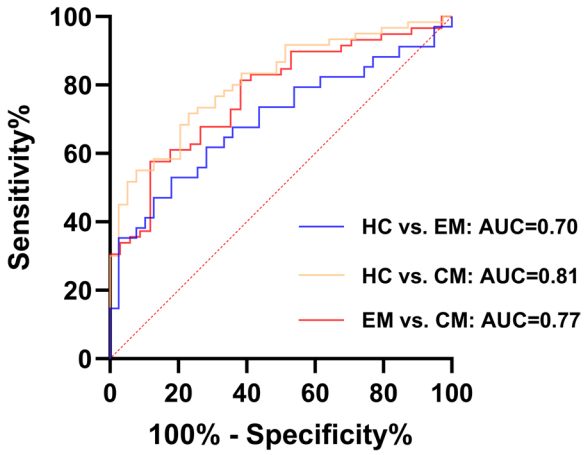

Fig. 6 The receiver operating characteristic (ROC) curve of the mean nodal local efficiency about significant group difference exhibited good performance to differentiate among HC, EM, and CM participants. AUC, area under the curve

ROC curve analysis

The receiver operating characteristic (ROC) curves of mean nodal local efficiency about significant group difference effectively distinguished HC, EM, and CM participants. Specifically, mean nodal local efficiency could differentiate EM from HC with an AUC of 0.70 ($p < 0.01$), CM from HC with an AUC of 0.81 ($p < 0.01$), and CM from EM with an AUC of 0.77 ($p < 0.01$) (Fig. 6). No significant results were found for the other network metrics tested.

Correlation analysis

Within the migraine patients, the characteristic path length and local efficiency were significantly correlated with the MIDAS scores (characteristic path length: r = 0.38, $p = 0.0003$; local efficiency: r = −0.37, $p = 0.0004$). Moreover, the nodal local efficiency of left opercular part of inferior frontal gyrus and right middle frontal gyrus were significantly correlated with the attack frequency (left opercular part of inferior frontal gyrus: r = −0.35, $p = 0.0005$; right middle frontal gyrus: r = −0.37, $p = 0.0002$). All the *p*-values above were still significant after Bonferroni correction.

Discussion

In our study, we examined the topological alterations in the structural brain connectome of participants with EM and CM. Diminished global efficiency and increased characteristic path length was found in the CM group compared with the HC group, indicating a less efficient structural network and longer information transfer pathways. Both EM and CM groups exhibited significantly reduced local efficiency compared to HCs, with CM showing lower local efficiency than EM. Moreover, the CM group demonstrated significant reductions in local clustering coefficient and nodal local efficiency in frontal and temporal brain regions compared to HCs and EM group. Nodal local efficiency effectively differentiated between CM, EM, and HC groups. Furthermore, the nodal local efficiency of specific brain regions, such as the left opercular part of the inferior frontal gyrus and right middle frontal gyrus, were negatively correlated with attack frequency. These findings align with the pathophysiology, implicating frontal and temporal lobe brain networks in anxiety, depression, and pain modulation in migraine [11].

Previous studies have laid the groundwork for understanding the intricate details of white matter microstructural imaging in the context of migraine with voxelwise approaches [30]. Yu et al. have found that

patients with EM showed significantly lower FA in several brain regions, including the subcortical white matter of frontal lobe, temporal lobe, and parietal lobe [12]. Similarly, another study using tract-based spatial statistics (TBSS) analysis revealed widespread increases in radial diffusivity (RD) and mean diffusivity (MD) values in the CM group compared to HCs [13].. In our study, the NBS analysis revealed distinct reductions in FA connectivity components in both EM and CM groups compared to HCs, showcasing specific nodes and connections implicated in each condition. While both patients with CM and EM exhibited micro-structural damage, as measured by TBSS, graph theory analysis revealed that patients with CM displayed greater significant alterations at the network level. Similarly, examining global topological network features in the context of the chronification of migraine, individuals with CM exhibited significant alterations compared to control participants. In contrast, those with EM showed minimal abnormalities. Based on our findings and existing literature, we propose that the chronification of migraine is not solely attributable to micro-structural alterations in white matter. Instead, it is suggested that a severe disruption of structural connections between brain areas, forming a network, is necessary to induce changes in information integration and organization, leading to migraine chronification.

Recent studies have highlighted the structural and functional connectivity alterations in migraine, revealing critical insights into its pathophysiology. For instance, Michels et al. observed that migraine patients exhibited a more segregated network topology, with CM patients showing greater modularity compared to EM, suggesting maladaptive reorganization in headache-related brain circuits [31, 32]. Similarly, Dai et al. reported enhanced integration and efficiency in global network properties among EM patients, correlating with clinical measures such as disease duration and headache impact scores [33]. In CM, DeSouza et al. found reduced global and local efficiency alongside increased segregation, with disruptions prominently in the limbic and insular cortices [34]. Structural network alterations extending to pain processing and modulation regions, such as the posterior cingulate and inferior parietal lobule, were further emphasized by Silvestro et al., who introduced a connectopathy model for migraine [35]. Li et al. focused on the vulnerability of rich-club regions, which showed increased feeder connection density in migraine patients, enhancing integration within pain-related circuits [36]. Lastly, Planchuelo-Gómez et al. underscored the coexistence of strengthened subcortical and weakened cortical connections in migraine, providing a nuanced understanding of structural connectivity changes [31]. These findings collectively underscore the importance of investigating global and regional network properties to elucidate the mechanisms underlying migraine chronification and progression. Moreover, recent studies on migraine-related brain networks have provided critical insights into the pathophysiological mechanisms of chronic migraine. Hosp et al. utilized DTI-based global tractography to construct the migraine-related pain network, identifying the insular cortex as a central hub connecting sensory, cognitive, and modulatory pathways, with white matter tract integrity closely linked to self-reported pain levels [37]. Borsook et al. highlighted the importance of subliminal neural dynamics and unconscious brain reorganization preceding chronic pain, suggesting that early interventions could mitigate the transition to chronic pain states [38]. These findings support the present study and further validate the critical role of disrupted structural network efficiency in chronic migraine.

Examining functional connectomes, a magnetoencephalographic study revealed reduced total node strength within pain-related cortical regions (bilateral primary and secondary somatosensory cortices, insula, medial frontal cortex, and anterior cingulate cortex) in CM patients, particularly in the beta band, compared to controls [39]. Notably, negative correlations between attack frequency and node strength were evident in the bilateral anterior cingulate cortex across all migraine patients. In another resting-state functional MRI study, Lee et al. have proposed that patients with CM exhibit enhanced connectivity within the pain matrix compared to those patients with EM [40]. The functional modifications observed in the pain network could contribute to the process of migraine chronification. These functional imaging findings complement our structural network analysis, emphasizing the involvement of frontal, parietal, and temporal lobes in migraine and its chronification.

The global impairment of structural connectivity in individuals with migraine (especially CM) was further supported by the presence of extensively distributed edges exhibiting reduced FA values in CM patients compared to HC participants and patients with EM. The observed decrease in global efficiency and increased characteristic path length in patients with CM suggests disrupted global information transfer and network integration. This aligns with findings in previous DTI studies about migraine, emphasizing the importance of global network properties in understanding headache disorders. The network-based analysis reveals specific alterations in FA values within connected sub-networks. The regions affected in EM and CM groups include brain regions associated with sensory processing and emotions [5]. The involvement of subcortical nuclei (thalamus and basal ganglia) and cortical regions in CM further emphasizes the widespread impact on structural connectivity.

The identification of regions with less local clustering coefficient and nodal local efficiency in both EM and CM groups, particularly in temporal and superior frontal gyrus regions, suggests a disruption in local network organization. The local clustering coefficient is a crucial metric in network science, quantifying the degree of interconnectedness among neighbors of a node in a network [41, 42]. For each node, the local clustering coefficient reflects the extent to which its neighbors form tightly connected clusters, calculated as the ratio of the actual number of edges between the node's neighbors to the maximum possible number of edges. Moreover, in our study, we observed significant group differences in the local clustering coefficient of two brain regions—left middle frontal gyrus, and right dorsolateral part of the superior frontal gyrus (left middle frontal gyrus: HC > EM; left middle frontal gyrus and right dorsolateral part of the superior frontal gyrus: HC > CM; right dorsolateral part of the superior frontal gyrus: EM > CM). These findings suggest that the prefrontal and superior frontal regions, particularly right dorsolateral part of the superior frontal gyrus, exhibit distinct alterations in local clustering patterns during the chronification of migraines. In a functional MRI study, Kong et al. found that in response to high pain stimuli, both the superior frontal gyrus and middle frontal gyrus exhibit significantly increased fMRI signal, suggesting their active involvement in processing and responding to intense pain stimuli [43]. Moreover, Mayr et al. found that in CM, the superior frontal gyrus exhibits reduced activity with increasing pain, indicating its involvement in the altered neural responses associated with CM conditions [44].

Nodal local efficiency is another pivotal metric in network neuroscience, offering insights into the efficiency of information transfer within specific brain regions [45, 46]. Moreover, in our study, we observed significant group differences in the nodal local efficiency of six brain regions—left gyrus rectus, right dorsolateral part of the superior frontal gyrus, right middle frontal gyrus, left opercular part of the inferior frontal gyrus, left hippocampus, and left inferior temporal gyrus (left gyrus rectus, right dorsolateral part of the superior frontal gyrus: HC > EM; left gyrus rectus, right dorsolateral part of the superior frontal gyrus, right middle frontal gyrus, left opercular part of the inferior frontal gyrus, left hippocampus, and left inferior temporal gyrus: HC > CM; right middle frontal gyrus, left opercular part of the inferior frontal gyrus, left hippocampus, and left inferior temporal gyrus: EM > CM). Previous studies have already demonstrated the role of right middle frontal gyrus, left opercular part of the inferior frontal gyrus, left hippocampus, and left inferior temporal gyrus in pain and emotions processing [47–51]. We speculated that the lower efficient information processing of pain circuit within the frontal and temporal lobe may be a biomarker of migraine chronification. This conclusion is consistent with the ROC analysis in which, mean nodal local efficiency about significant group difference exhibited good performance to differentiate among EM and CM participants.

Moreover, the observed negative correlation between local efficiency and MIDAS scores among migraine patients suggests a meaningful connection between changes in local network metrics and the clinical severity of migraine. This association underscores the profound impact of network disruptions on the extent of migraine-related disability, providing deeper insights into the intricate relationship between brain network alterations and the diseases progression of migraine. We also found that the nodal local efficiency of left opercular part of inferior frontal gyrus and right middle frontal gyrus were negatively correlated with the headache attack frequency, which means the disrupted network efficiency of the two regions are significantly associated with migraine chronification.

This study has several strengths and novel contributions. Unlike previous studies that focus on either EM or CM, it comprehensively compares CM, EM, and HCs, revealing distinct structural connectivity disruptions linked to migraine chronification. By integrating multiple graph metrics, such as global/local efficiency and clustering coefficient, this work highlights topological changes, particularly in the frontal and temporal regions, as specific markers of chronification. Moreover, the associations between these disrupted metrics and clinical features, such as MIDAS scores and attack frequency, enhance its clinical relevance. However, it is important to acknowledge that our study, while providing valuable insights, is not without its limitations. First, this study is an observational study with a cross-sectional design. Cross-sectional studies capture data at a single time point, providing only a snapshot of the disease state. This approach does not account for the temporal dynamics of disease progression or the potential bidirectional relationships between observed network changes and clinical outcomes. Suggest the need for longitudinal studies to identify early imaging markers for disease prediction. Second, the study did not control for the phase of migraine (ictal or interictal) during MRI scanning, which could potentially influence the results. Third, future research should also explore multimodal imaging approaches that combine structural and functional MRI to gain a more comprehensive understanding of the structural and functional changes in migraine [52]. Fourth, while our study primarily focused on cerebral regions, the cerebellum also plays an important role in

pain modulation in migraine [53]. This could be considered a limitation, and future research should investigate the involvement of the cerebellum in chronic migraine. Fifth, the choice of using DTI for tractography in this study may not fully capture complex fiber configurations, particularly in regions with crossing fibers. More advanced fiber modeling techniques, such as constrained spherical deconvolution (CSD) or the ball-and-stick model, could provide a more accurate depiction of fiber orientation distributions [54]. Future studies should employ advanced tractography methods to enhance the reliability of connectomic analyses.

Conclusion

This study provides significant insights into the structural brain networks of migraine patients, particularly highlighting the disruptions in both global and local properties. Our findings suggest that CM is associated with decreased global efficiency, increased characteristic path length, and reduced local efficiency, which are indicative of compromised structural connectivity and information transfer within the brain. These alterations were more pronounced in CM patients compared to those with EM and HCs, emphasizing the severity of network disruptions in chronic migraine. Furthermore, our analysis identified specific reductions in local clustering coefficient and nodal local efficiency in the frontal and temporal brain regions of CM patients. These metrics effectively differentiated between CM, EM, and HC groups, underscoring their potential as neuroimaging markers for migraine chronification. The observed negative correlations between nodal local efficiency and attack frequency, particularly in the left opercular part of the inferior frontal gyrus and the right middle frontal gyrus, further support the role of these regions in the pathophysiology of migraine.

These findings offer valuable diagnostic markers and underscore the importance of network-based metrics in understanding and characterizing migraine-related structural alterations. By integrating these network metrics into clinical practice, there is potential for improved migraine classification and personalized treatment approaches. Future research should focus on longitudinal studies to validate these findings and explore the integration of multimodal imaging techniques to gain a comprehensive understanding of both structural and functional changes in migraine.

Consent for publication

All authors consent for the publication.

Abbreviations

Analysis of variance	ANOVA
CM	Chronic migraine
EM	Episodic migraine
HCs	Healthy controls
DTI	Diffusion tensor imaging
ICHD-3	International Classification of Headache Diseases, Third Edition
MRI	Magnetic resonance imaging
BMI	Body mass index
VAS	Visual Analogue Scale
PHQ-9	Patient Health Questionnaire-9
HIT-6	Headache Impact Test-6
GAD-7	Generalized Anxiety Disorder-7
PSQI	Pittsburgh Sleep Quality Index
FA	Fractional anisotropy
AAL	Automated Anatomical Labeling
SD	Standard deviation
FDR	False discovery rate
NBS	Network-based statistic
ROC	Receiver operating characteristic curve
TBSS	Tract-based spatial statistics
RD	Radial diffusivity
MD	Mean diffusivity

Acknowledgements

We extend our sincere gratitude to the National Neurological Imaging Centre of Beijing Tiantan Hospital, Capital Medical University, for their invaluable technical and equipment support throughout this study. Additionally, we express our heartfelt appreciation to the headache specialists whose expertise was instrumental in ensuring accurate diagnoses.

Authors' contributions

The study was conceptualized and designed by YLM, HFT, and YGW. DQ and YLM conducted the initial data analysis. YLM and DQ oversaw data quality control measures. All authors participated in clinical and MRI data collection. YLM drafted the initial manuscript, which was critically reviewed and revised by all authors until consensus on the final version was reached.

Funding

This research was funded by the National Natural Science Foundation of Beijing (Z200024) and the National Natural Science Foundation of China (grant numbers 32170752, 31770800, and 91849104).

Data availability

Data can be made available upon request.

Declarations

Consent for publication

All authors consent for the publication.

Competing interests

The authors declare no competing interests.

Author details

[1]Headache Center, Department of Neurology, Beijing Tiantan Hospital, Capital Medical University, Beijing, China. [2]Tiantan Neuroimaging Center of Excellence, China National Clinical Research Center for Neurological Diseases, Beijing, China. [3]Department of Radiology, Beijing Tiantan Hospital, Capital Medical University, Beijing Neurosurgical Institute, Beijing, China. [4]Department of Neurology, Shenzhen Second People's Hospital, Shenzhen, Guangdong 518000, China. [5]Department of Neurology, The First Affiliated Hospital of Dalian Medical University, Dalian, Liaoning, China.

Received: 8 October 2024 Accepted: 18 November 2024
Published online: 25 November 2024

References

1. Dodick DW (2018) Migraine[J]. Lancet 391(10127):1315–1330. https://doi.org/10.1016/s0140-6736(18)30478-1

2. Ashina M (2020) Migraine[J]. N Engl J Med 383(19):1866–1876. https://doi.org/10.1056/NEJMra1915327
3. Steiner TJ, Stovner LJ (2023) Global epidemiology of migraine and its implications for public health and health policy[J]. Nat Rev Neurol 19(2):109–117. https://doi.org/10.1038/s41582-022-00763-1
4. Stovner LJ, Hagen K, Linde M et al (2022) The global prevalence of headache: an update, with analysis of the influences of methodological factors on prevalence estimates[J]. J Headache Pain 23(1):34. https://doi.org/10.1186/s10194-022-01402-2
5. May A, Schulte LH (2016) Chronic migraine: risk factors, mechanisms and treatment[J]. Nat Rev Neurol 12(8):455–464. https://doi.org/10.1038/nrneurol.2016.93
6. Schwedt TJ (2014) Chronic migraine[J]. BMJ 348:g1416. https://doi.org/10.1136/bmj.g1416
7. Filippi M, Messina R (2019) The Chronic Migraine Brain: What Have We Learned From Neuroimaging?[J]. Front Neurol 10:1356. https://doi.org/10.3389/fneur.2019.01356
8. Torres-Ferrús M, Ursitti F, Alpuente A et al (2020) From transformation to chronification of migraine: pathophysiological and clinical aspects[J]. J Headache Pain 21(1):42. https://doi.org/10.1186/s10194-020-01111-8
9. Katsarava Z, Buse DC, Manack AN et al (2012) Defining the differences between episodic migraine and chronic migraine[J]. Curr Pain Headache Rep 16(1):86–92. https://doi.org/10.1007/s11916-011-0233-z
10. Lee CH, Park H, Lee MJ et al (2023) Whole-brain functional gradients reveal cortical and subcortical alterations in patients with episodic migraine[J]. Hum Brain Mapp 44(6):2224–2233. https://doi.org/10.1002/hbm.26204
11. Dai W, Liu RH, Qiu E et al (2021) Cortical mechanisms in migraine[J]. Mol Pain 17:17448069211050246. https://doi.org/10.1177/17448069211050246
12. Yu D, Yuan K, Qin W et al (2013) Axonal loss of white matter in migraine without aura: a tract-based spatial statistics study[J]. Cephalalgia 33(1):34–42. https://doi.org/10.1177/0333102412466964
13. Coppola G, Di Renzo A, Tinelli E et al (2020) Patients with chronic migraine without history of medication overuse are characterized by a peculiar white matter fiber bundle profile[J]. J Headache Pain 21(1):92. https://doi.org/10.1186/s10194-020-01159-6
14. Gomez-Beldarrain M, Oroz I, Zapirain BG et al (2015) Right fronto-insular white matter tracts link cognitive reserve and pain in migraine patients[J]. J Headache Pain 17:4. https://doi.org/10.1186/s10194-016-0593-1
15. Cao M, Wang JH, Dai ZJ et al (2014) Topological organization of the human brain functional connectome across the lifespan[J]. Dev Cogn Neurosci 7:76–93. https://doi.org/10.1016/j.dcn.2013.11.004
16. Sporns O (2013) Structure and function of complex brain networks[J]. Dialogues Clin Neurosci 15(3):247–262. https://doi.org/10.31887/DCNS.2013.15.3/osporns
17. Schwedt TJ, Nikolova S, Dumkrieger G et al (2022) Longitudinal changes in functional connectivity and pain-induced brain activations in patients with migraine: a functional MRI study pre- and post- treatment with Erenumab[J]. J Headache Pain 23(1):159. https://doi.org/10.1186/s10194-022-01526-5
18. Liu J, Zhao L, Lei F et al (2015) Disrupted resting-state functional connectivity and its changing trend in migraine suffers[J]. Hum Brain Mapp 36(5):1892–1907. https://doi.org/10.1002/hbm.22744
19. Headache Classification Committee of the International Headache Society (IHS) The International Classification of Headache Disorders, 3rd edition[J]. Cephalalgia, 2018, 38(1): 1–211.https://doi.org/10.1177/0333102417738202
20. Negeri ZF, Levis B, Sun Y et al (2021) Accuracy of the Patient Health Questionnaire-9 for screening to detect major depression: updated systematic review and individual participant data meta-analysis[J]. BMJ 375:n2183. https://doi.org/10.1136/bmj.n2183
21. Löwe B, Decker O, Müller S et al (2008) Validation and standardization of the Generalized Anxiety Disorder Screener (GAD-7) in the general population[J]. Med Care 46(3):266–274. https://doi.org/10.1097/MLR.0b013e318160d093
22. Li J, Yao YS, Dong Q et al (2013) Characterization and factors associated with sleep quality among rural elderly in China[J]. Arch Gerontol Geriatr 56(1):237–243. https://doi.org/10.1016/j.archger.2012.08.002
23. Mori S, Crain BJ, Chacko VP et al (1999) Three-dimensional tracking of axonal projections in the brain by magnetic resonance imaging[J]. Ann Neurol 45(2):265–269. https://doi.org/10.1002/1531-8249(199902)45:2%3c265::aid-ana21%3e3.0.co;2-3
24. Lu FM, Dai J, Couto TA et al (2017) Diffusion Tensor Imaging Tractography Reveals Disrupted White Matter Structural Connectivity Network in Healthy Adults with Insomnia Symptoms[J]. Front Hum Neurosci 11:583. https://doi.org/10.3389/fnhum.2017.00583
25. Tzourio-Mazoyer N, Landeau B, Papathanassiou D et al (2002) Automated anatomical labeling of activations in SPM using a macroscopic anatomical parcellation of the MNI MRI single-subject brain[J]. Neuroimage 15(1):273–289. https://doi.org/10.1006/nimg.2001.0978
26. Fonov V, Evans AC, Botteron K et al (2011) Unbiased average age-appropriate atlases for pediatric studies[J]. Neuroimage 54(1):313–327. https://doi.org/10.1016/j.neuroimage.2010.07.033
27. Kwon H, Choi YH, Seo SW et al (2017) Scale-integrated Network Hubs of the White Matter Structural Network[J]. Sci Rep 7(1):2449. https://doi.org/10.1038/s41598-017-02342-7
28. Fu T, Gao Y, Huang X et al (2024) Brain connectome-based imaging markers for identifiable signature of migraine with and without aura[J]. Quant Imaging Med Surg 14(1):194–207. https://doi.org/10.21037/qims-23-827
29. Zalesky A, Fornito A, Bullmore ET (2010) Network-based statistic: identifying differences in brain networks[J]. Neuroimage 53(4):1197–1207. https://doi.org/10.1016/j.neuroimage.2010.06.041
30. Rahimi R, Dolatshahi M, Abbasi-Feijani F et al (2022) Microstructural white matter alterations associated with migraine headaches: a systematic review of diffusion tensor imaging studies[J]. Brain Imaging Behav 16(5):2375–2401. https://doi.org/10.1007/s11682-022-00690-1
31. Planchuelo-Gómez Á, García-Azorín D, Guerrero ÁL et al (2020) Structural connectivity alterations in chronic and episodic migraine: A diffusion magnetic resonance imaging connectomics study[J]. Cephalalgia 40(4):367–383. https://doi.org/10.1177/0333102419885392
32. Michels L, Koirala N, Groppa S et al (2021) Structural brain network characteristics in patients with episodic and chronic migraine[J]. J Headache Pain 22(1):8. https://doi.org/10.1186/s10194-021-01216-8
33. Dai L, Zheng Q, Chen X et al (2021) Altered brain structural topological properties and its correlations with clinical characteristics in episodic migraine without aura[J]. Neuroradiology 63(12):2099–2109. https://doi.org/10.1007/s00234-021-02716-9
34. DeSouza DD, Woldeamanuel YW, Sanjanwala BM et al (2020) Altered structural brain network topology in chronic migraine[J]. Brain Struct Funct 225(1):161–172. https://doi.org/10.1007/s00429-019-01994-7
35. Silvestro M, Tessitore A, Caiazzo G et al (2021) Disconnectome of the migraine brain: a "connectopathy" model[J]. J Headache Pain 22(1):102. https://doi.org/10.1186/s10194-021-01315-6
36. Li K, Liu L, Yin Q et al (2017) Abnormal rich club organization and impaired correlation between structural and functional connectivity in migraine sufferers[J]. Brain Imaging Behav 11(2):526–540. https://doi.org/10.1007/s11682-016-9533-6
37. Hosp JA, Reisert M, von Kageneck C et al (2021) Approximation to pain-signaling network in humans by means of migraine[J]. Hum Brain Mapp 42(3):766–779. https://doi.org/10.1002/hbm.25261
38. Borsook D, Youssef AM, Barakat N et al (2018) Subliminal (latent) processing of pain and its evolution to conscious awareness[J]. Neurosci Biobehav Rev 88:1–15. https://doi.org/10.1016/j.neubiorev.2018.02.015
39. Hsiao FJ, Chen WT, Liu HY et al (2021) Migraine chronification is associated with beta-band connectivity within the pain-related cortical regions: a magnetoencephalographic study[J]. Pain 162(10):2590–2598. https://doi.org/10.1097/j.pain.0000000000002255
40. Lee MJ, Park BY, Cho S et al (2019) Increased connectivity of pain matrix in chronic migraine: a resting-state functional MRI study[J]. J Headache Pain 20(1):29. https://doi.org/10.1186/s10194-019-0986-z
41. Koutrouli M, Karatzas E, Paez-Espino D et al (2020) A Guide to Conquer the Biological Network Era Using Graph Theory[J]. Front Bioeng Biotechnol 8:34. https://doi.org/10.3389/fbioe.2020.00034
42. Chen Q, Baran TM, Turnbull A et al (2021) Increased segregation of structural brain networks underpins enhanced broad cognitive abilities of cognitive training[J]. Hum Brain Mapp 42(10):3202–3215. https://doi.org/10.1002/hbm.25428
43. Kong J, Loggia ML, Zyloney C et al (2010) Exploring the brain in pain: activations, deactivations and their relation[J]. Pain 148(2):257–267. https://doi.org/10.1016/j.pain.2009.11.008

44. Mayr A, Jahn P, Stankewitz A et al (2022) Patients with chronic pain exhibit individually unique cortical signatures of pain encoding[J]. Hum Brain Mapp 43(5):1676–1693. https://doi.org/10.1002/hbm.25750
45. Ma X, Jiang G, Fu S et al (2018) Enhanced Network Efficiency of Functional Brain Networks in Primary Insomnia Patients[J]. Front Psychiatry 9:46. https://doi.org/10.3389/fpsyt.2018.00046
46. Li C, Qiao K, Mu Y et al (2021) Large-Scale Morphological Network Efficiency of Human Brain: Cognitive Intelligence and Emotional Intelligence[J]. Front Aging Neurosci 13:605158. https://doi.org/10.3389/fnagi.2021.605158
47. Aasted CM, Yücel MA, Steele SC et al (2016) Frontal Lobe Hemodynamic Responses to Painful Stimulation: A Potential Brain Marker of Nociception[J]. PLoS ONE 11(11):e0165226. https://doi.org/10.1371/journal.pone.0165226
48. Bonanno L, Lo Buono V, De Salvo S et al (2020) Brain morphologic abnormalities in migraine patients: an observational study[J]. J Headache Pain 21(1):39. https://doi.org/10.1186/s10194-020-01109-2
49. Liu HY, Chou KH, Chen WT (2018) Migraine and the Hippocampus[J]. Curr Pain Headache Rep 22(2):13. https://doi.org/10.1007/s11916-018-0668-6
50. Maleki N, Becerra L, Brawn J et al (2013) Common hippocampal structural and functional changes in migraine[J]. Brain Struct Funct 218(4):903–912. https://doi.org/10.1007/s00429-012-0437-y
51. Qin Z, Su J, He XW et al (2020) Disrupted functional connectivity between sub-regions in the sensorimotor areas and cortex in migraine without aura[J]. J Headache Pain 21(1):47. https://doi.org/10.1186/s10194-020-01118-1
52. Fotiadis P, Parkes L, Davis KA et al (2024) Structure-function coupling in macroscale human brain networks[J]. Nat Rev Neurosci 25(10):688–704. https://doi.org/10.1038/s41583-024-00846-6
53. Mehnert J, May A (2019) Functional and structural alterations in the migraine cerebellum[J]. J Cereb Blood Flow Metab 39(4):730–739. https://doi.org/10.1177/0271678x17722109
54. Calamante F. The Seven Deadly Sins of Measuring Brain Structural Connectivity Using Diffusion MRI Streamlines Fibre-Tracking[J]. Diagnostics (Basel), 2019, 9(3).https://doi.org/10.3390/diagnostics9030115

Publisher's Note